

## Comparative Study on the NO<sub>2</sub> Bindings to (MgO)<sub>n</sub> and (CaO)<sub>n</sub> Clusters, n = 4, 6, and 9: Formation of Nitrite and Nitrate

FATHI HASSAN BAWA

*Department of Physics, Faculty of Science, Seventh of October University, Misurata, Libya.*

(Received on 8<sup>th</sup> June 2009, accepted in revised form 15<sup>th</sup> February 2010)

**Summary:** A comparative study on MgO and CaO clusters toward NO<sub>2</sub> adsorption have been investigated theoretically by the density functional theory, approach Beck3LYP. Bond lengths, bond angles as well as adsorption energies of the MgO-NO<sub>2</sub> and CaO-NO<sub>2</sub> modes are calculated for varieties of sites on the three model clusters. The results indicated that there is a weak bound involving the (MgO)<sub>9</sub> cluster to the magnesium cations at face site (0.32 eV) and edge site (0.36 eV), and found sensitive to the size of the cluster that (0.87 eV) and (1.23 eV) are obtained for (MgO)<sub>6</sub> and (MgO)<sub>4</sub>, respectively. In contrast, the binding stabilities for NO<sub>2</sub> towards surface nitrite formation reveal significantly different (1.37 eV) and (1.66 eV) are obtained for (CaO)<sub>4</sub>, and (CaO)<sub>9</sub> clusters respectively. The NO<sub>2</sub> adsorption was found also reactive on (CaO)<sub>9</sub> forming nitrate species, and present slightly large binding energy compared to (MgO)<sub>9</sub> clusters. The reason for the difference in binding energies is discussed in terms of cluster electro-positivity, and the nature of the highest occupied molecular orbital. NO<sub>3</sub><sup>2-</sup> surface species is also characterized.

### Introduction

Nanotechnology, might give us better ways of trapping solar energy, harnessing a renewable natural resource that would replace the fossil fuel in order to meet clean air regulations. In this context, a catalytic solid surface is used in order to control emissions and to enhance the result of the synthetic route. Nanoparticles may constitute nanofilters for instant removing pollution from rivers and lakes. Nanotechnology leads to the development of nanotubes, which are made of carbon atoms, are very light and much stronger than steel, and also conduct heat and electricity. Considering the metal oxide surfaces, the bond between the NO<sub>2</sub> molecules and metal oxide is particularly very important as it may provide information about the molecule-metal oxide interactions and the resulting binding strength. It is well known that, nitrogen oxides are a group of gases produced by the combustions of fossil fuels, especially when combustion takes place at high temperatures and pressures. Direct emissions are mainly in the form of nitric oxide NO with amounts of nitrogen dioxide NO<sub>2</sub> and nitrous oxide N<sub>2</sub>O. Nitric oxide and nitrogen dioxide are often lumped together as NO<sub>x</sub>. The last three decade has seen a remarkable change in the way that we perceive the oxide materials. Transition metal oxides have been reported to display complex chemical properties as observed by means of electrochemistry leading to a new electro-catalytical branch of research, which aims to identify the detailed molecule-electrode interactions. Furthermore, a reassessment of the

technological importance of the simple alkaline earth oxides is currently taking place. Particularly, focus has been the identification of material oxides such as MgO and CaO clusters to reduce NO<sub>2</sub> emissions. Thus due to this reason, nitrogen oxides emissions may be controlled by a variety of processes. This awareness has reached the political stage on the global arena and it may very soon lead to actions to monitor and control emissions of gases pollutants. Ways in which this can be achieved include the use of exhaust treatment catalysts.

The "lean-burn automotive engine" project is characteristic of the issues that become critical when environmentally friendly fuel efficiency is sought [1-4]. It has long been known that reduction of fuel consumption in conventional automotive vehicles required operating the engine at high air to fuel ratios in order to approach complete combustion. At such lean conditions however, the concentrations of environmentally hazardous nitrogen oxides NO<sub>x</sub> increase, which necessitate development of efficient catalysts for NO<sub>x</sub> reduction. Thus, surface of Ba (NO<sub>3</sub>)<sub>2</sub> and Pt are precipitated on an alumina support, forming the Pt-BaO/Al<sub>2</sub>O<sub>3</sub> catalyst by subsequent calcinations. The role of the Pt/Al<sub>2</sub>O<sub>3</sub> substrate is to catalyze low temperature conversion of NO to NO<sub>2</sub>, which is subsequently absorbed in the BaO/Al<sub>2</sub>O<sub>3</sub> component [5]. During short periods of fuel rich conditions, NO<sub>2</sub> is released from the substrate, and seen to act as oxidant in the fuel combustion,

whereby effectively all NO<sub>2</sub> associated nitrogen is converted into N<sub>2</sub>. The gas absorption properties of the metal oxides and also their reduction properties are considered crucial. The relevant quantum chemical studies in this context have focused mainly on the oxide surface chemistry. Thus, direct catalytic NO and NO<sub>2</sub> reductions on the CaO (100) surface at terrace and step sites have been addressed by means of theory [6]. This study includes also N<sub>2</sub>O decomposition over CaO [7], and formation of the hyponitrite ion N<sub>2</sub>O<sub>2</sub><sup>2-</sup> [8]. Storage mechanisms of NO<sub>2</sub> on alkaline earth oxides have been the subject of some recent investigations MgO(s) [9, 10] and BaO (100) [11, 12, 13]. Indeed, presently, the focus is shifting from single crystal studies and films, as increasingly more intriguing properties are revealed related to the fact that some 20% discrepancy to the bulk stability remains for quite large clusters.

The distinction between cluster and bulk regarding binding energies and structures was elucidated previously for the (MO)<sub>n</sub> clusters, where M denotes Mg and Ca, and 2 ≤ n ≤ 12 [14]. Furthermore, topologically equivalent clusters were found to display similar stabilities [15], implying rapid convergence of binding energy per MO unit towards the binding energy of an infinite metal oxide sheet.

The present contribution addresses differential properties of (MgO)<sub>n</sub> and (CaO)<sub>n</sub> cluster models regarding the chemisorptions of NO<sub>2</sub> molecule, while a subsequent study will address the pair-wise chemisorption mechanism of NO<sub>2</sub> onto (MgO)<sub>9</sub> and (CaO)<sub>9</sub>, and suggested an enhancement the NO<sub>2</sub> chemisorption on MgO (001) [9].

In this work DFT are used to study of NO<sub>2</sub> adsorption and storage on alkaline earth oxide. The reactive adsorbed tendencies are compared and the role of the oxide surface has been elaborated.

#### Computational Details

The present study employs the B3LYP hybrid density functional [16-18] as implemented in the GAUSSIAN 98 program suite [19]. This is thoroughly tested effective description of the exchange-correlation potential for which wide experience of its performance has been acquired. In particular, it is known to perform well for small molecules. The exceptions are found in the systems

where the Kohn-Sham density cannot be the true density, *e.g.*, when there exists near-degenerate independent particle states of the same spin and space symmetry. In such pathological systems, the whole ensemble of states must be explicitly included in the wave function in order to produce the true density [20].

Balances, and cost efficiency has guided the choice of basis sets for the atoms. Semi-quantitative absolute results are aimed for, but even more, so the present study seeks to point at differential effects. In case of N and O, the 6-31+G(d) set was used except for some stability tests using the 6-311G(d) set. In case of Mg and Ca, the 6-311G basis set was used throughout. For Ca this acronym implies the inclusion one d-function. Different cluster models were employed depending on the size of cluster and the position of the adsorbate molecule. For MgO, we employed three cluster models (MgO)<sub>4</sub> (cube structure) (MgO)<sub>6</sub>, and (MgO)<sub>9</sub> (2-hexagonal ring stacks) and (3-hexagonal ring stacks), respectively. While two models of (CaO)<sub>4</sub> (Cube) and (CaO)<sub>9</sub> (3-hexagonal ring stacks) were employed as well. Adsorption energies were calculated for slab and cylinder shapes using the expression

$$\Delta E_{\text{ads}} = E_{\text{NO}_2} + E_{\text{cylinder}} - E_{(\text{NO}_2+\text{cylinder})} \quad (1)$$

$$\Delta E_{\text{ads}} = E_{\text{NO}_2} + E_{\text{slab}} - E_{(\text{NO}_2+\text{slab})} \quad (2)$$

#### Results and Discussion

##### NO<sub>2</sub> Adsorption to MO Clusters-Conceptual Understanding of Two Species

On a material oxide cluster, NO<sub>2</sub> chemisorption can occur on either the metal cations or the oxygen anions. Adsorption to the metal cation is straightforward. Initially the NO<sub>2</sub> molecule attaches to the cation by an ion-to-dipole attractive interaction. Enhancement of the native electron affinity of the NO<sub>2</sub> molecule by the M<sup>2+</sup> field, makes NO<sub>2</sub> a competitive electron sink even when compared to the cluster O<sup>2-</sup> anions. A surface nitrite is formed (Fig. 1 (a)).

Adsorption of NO<sub>2</sub> on a substrate oxygen is less chemically intuitive, since it involves the formation of an NO<sub>3</sub><sup>2-</sup> species. A chemical understanding of how such a species can become stable at an oxide surface is drawn schematically in

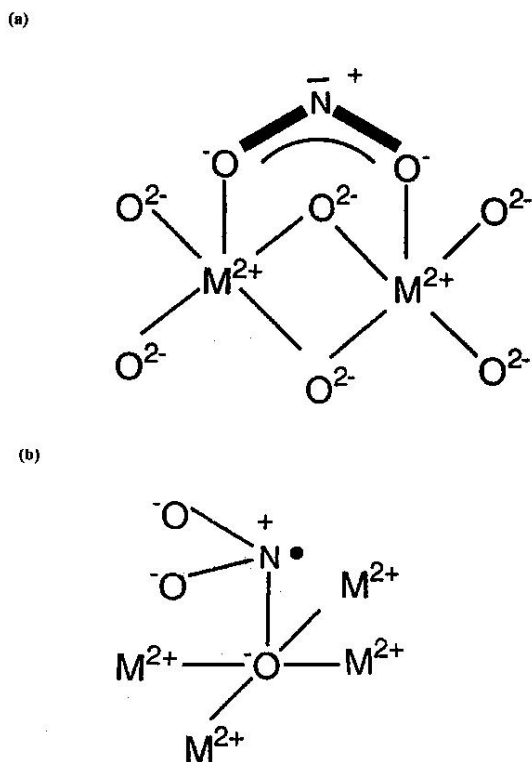


Fig. 1: Schematic view for the  $\text{NO}_2$  on two  $\text{M}^{2+}$  cations and single oxide anion  $\text{O}^{2-}$  sites of  $\text{MgO}$  and  $\text{CaO}$  clusters to form two surface species, (a)  $\text{NO}_2^-$  and (b)  $\text{NO}_3^{2-}$ .

Fig. 1(b) implications to the mechanism for nitrate formation on alkaline earth oxides is discussed further in [11].

Here, the singly highest occupied molecular orbitals (HOMOs) are employed in order to clarify further the difference between the two ways that  $\text{NO}_2$  may chemisorb to an oxide (see Fig. 2). In case of the  $\text{NO}_3^{2-}$  species, it is observed how the HOMO is localized mainly in the immediate adsorption region (Fig. 2 (b)). In contrast, for the more conventional bidentate  $\text{NO}_2^-$  nitrite-like adsorbate found at the  $\text{M}^{2+}$  site (see Fig. 1 (a)), a significantly more delocalized HOMO results is shown in Fig. 2 (a), which implies partial oxidation of the cluster oxygens.

In viewing an alkaline earth metal oxide as a positive charge reservoir, this tends to release electrons to form a chemical bond. The above consequence being a better illustrated the asymmetry in the ways a hole or electron is accommodated.

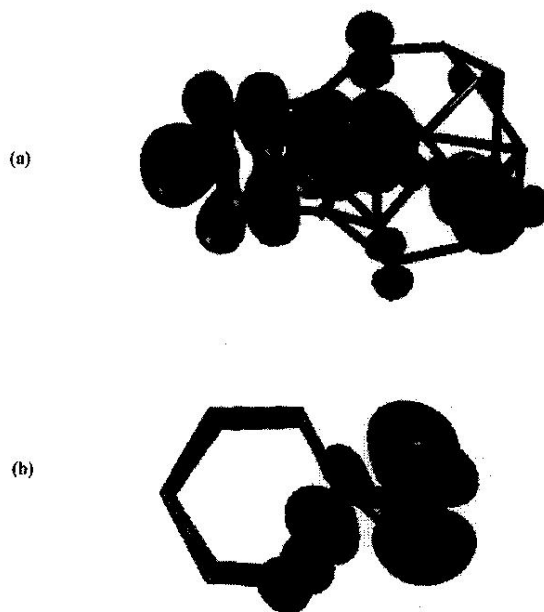


Fig. 2: HOMO for (a)  $\text{NO}_2^-$  (surface) and (b)  $\text{NO}_3^{2-}$  (surface). The HOMO is mainly delocalized and localized within the interfacial adsorption region at  $\text{NO}_2^-$  and  $\text{NO}_3^{2-}$ , respectively.

#### Structure and Energetics- $\text{NO}_2$ on $(\text{MgO})_n$ and $(\text{CaO})_n$ Clusters

Structural characteristics of  $\text{NO}_2$  adsorbed on  $(\text{MgO})_n$  and  $(\text{CaO})_n$  clusters are depicted in Fig. 3 and Fig. 4 respectively. Characteristic structural aspects of the nitrite and nitrate surface species are collected in (Tables-1 and 2), respectively. The pyramidal structure of the  $\text{NO}_3^{2-}$  surface species is in contrast to the  $\text{sp}^2$  hybridized planar  $\text{NO}_3^-$  ion, and the structure of the former is associated with,  $\text{sp}^3$  hybridization on the central nitrogen atom. This is in support of the understanding displayed in Fig. 1 (b), and consistent with the distribution of the HOMO (see Fig. 2 (a)). It becomes interesting to compare the stability of the surface  $\text{NO}_3^{2-}$  species on  $(\text{MgO})_9$ , in contrast to  $(\text{CaO})_9$  (cf. Fig. 3 and Fig. 4, and the  $E_{\text{ads}}$  values in Table- 2). We observe that both structural parameters and chemisorption energies come out fairly similar (0.36 eV) and (0.68 eV), respectively. In contrast, the binding energies for the bidentate nitrite ion are found to be very sensitive to the choice of cation. Hence, the  $\text{NO}_2^-$  binding energy to form  $\text{NO}_2^-$  is (0.36 eV) on  $(\text{MgO})_9$  as compared to (1.66

Table-1: Structural parameters and binding energies of bidentate binding of  $\text{NO}_2$  on  $(\text{MgO})_n$  ( $n = 4, 6$  and  $9$ ) and  $(\text{CaO})_n$  clusters,  $n = (4, 9)$ .

Structure	N-O	$\text{M}_i\text{-ONO}$	$\angle\text{O-N-O}$	$\angle\text{M}_i\text{-O-N}$	$E_{\text{ads}}$
Free $\text{NO}_2$					
6-31+G(d)	1.20	-	134°	-	-
311G(d)	1.19	-	134°	-	-
Exp. [Green]	1.20	-	134°	-	-
Free $\text{NO}_2^-$					
6-31+G(d)	1.26	-	116°	-	-
6-311G(d)	1.26	-	116°	-	-
$\text{NO}_2/(\text{MgO})_4$					
6-311G(d)	a=1.25 b=1.26	a=2.05 b=2.07	118°	$\alpha=129^\circ$ $\beta=127^\circ$	1.23
6-31+G(d)	a=1.26 b=1.27	a=2.06 b=2.08	117°	$\alpha=129^\circ$ $\beta=127^\circ$	1.11
$\text{NO}_2/(\text{MgO})_6$					
6-311G(d)	a=1.25 b=1.25	a=2.08 b=2.09	118°	$\alpha=128^\circ$ $\beta=129^\circ$	0.87
6-31+G(d)	a=1.26 b=1.26	a=2.08 b=2.08	118°	$\alpha=129^\circ$ $\beta=128^\circ$	0.69
$\text{NO}_2/(\text{MgO})_9$					
Face site					
6-31+G(d)	a=1.21 b=1.23	a=2.15 b=2.53	124°	$\alpha=118^\circ$ $\beta=130^\circ$	0.32
Edge site					
6-31+G(d)	a=1.24 b=1.24	a=2.19 b=2.35	122°	$\alpha=126^\circ$ $\beta=137^\circ$	0.36
$\text{NO}_2/(\text{CaO})_4$					
6-31+G(d)	a=1.25 b=1.25	a=2.36 b=2.37	116°	$\alpha=133^\circ$ $\beta=135^\circ$	1.37
$\text{NO}_2/(\text{CaO})_9$					
6-31+G(d)	a=1.25 b=1.27	a=2.37 b=2.50	115°	$\alpha=118^\circ$ $\beta=149^\circ$	1.66

N-O and  $\text{M}_i\text{-ONO}$  are the distances between the nitrogen atom and oxygen atom in a  $\text{NO}_2$  molecule, and the metal cation surface and oxygen distance, respectively.  $\alpha$  and  $\beta$  are angles, between two  $\text{M}_i$  cations and  $\text{NO}_2$  (see Figs. 3 and 4).  $E_{\text{ads}}$  is the adsorption energies in (eV), of  $\text{NO}_2$  on the  $(\text{MO})_n$ , where  $\text{M}=\text{Mg}$  and  $\text{Ca}$ . Distances are given in Å, and angles in degrees.

Table-2: Structure and stability of the  $\text{NO}_3^{2-}$  surface species on  $(\text{MgO})_9$  and  $(\text{CaO})_9$  clusters.

System	N-O	$\text{O}_{\text{surf}}\text{-N}$	$\angle\text{O-N-O}$	$\angle\text{O}_{\text{surf}}\text{-N-O}$	tilt angle	$E_{\text{ads}}$
$\text{NO}_2/(\text{MgO})_9$	1.30	1.45	125°	110°	133°	0.36
$\text{NO}_2/(\text{CaO})_9$	1.29	1.51	120°	110°	132°	0.68

eV) on  $(\text{CaO})_9$ . This substantial difference was confirmed by probing face site (0.32 eV) on the  $(\text{MgO})_9$  cluster. In order to learn more about the origin of this discrepancy, bidentate nitrite binding energies were also computed on the  $(\text{MgO})_4$ ,  $(\text{MgO})_6$  and  $(\text{CaO})_4$  clusters. Interestingly, the surface nitrite stability is found to diminish monotonously for  $(\text{MgO})_n$  where,  $n = 4, 6$  and  $9$  as (1.11 eV) (0.69 eV), and (0.36 eV) were computed respectively. In contrast, the stability of the nitrite ion is somewhat enhanced on going from  $(\text{CaO})_4$  to  $(\text{CaO})_9$ , in the range (1.37 to 1.66 eV). The structural parameters

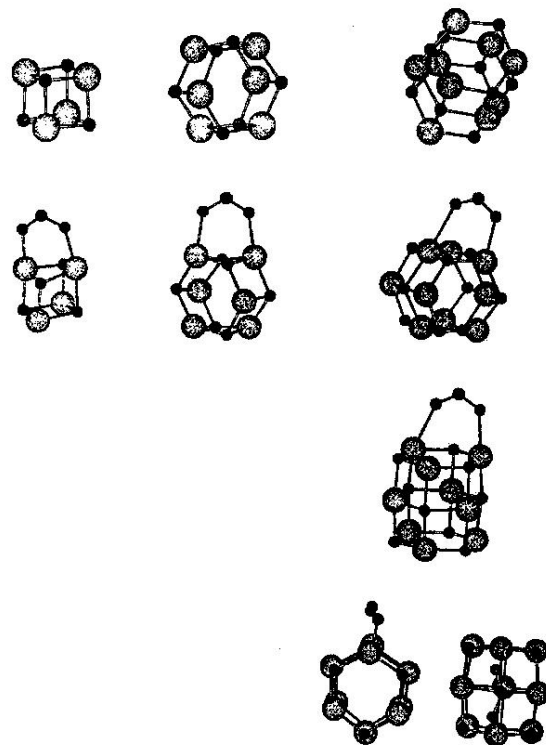


Fig. 3: Geometries and binding energies for  $\text{NO}_2$  @  $(\text{MgO})_n$ ,  $n = 4, 6, 9$ . Two perspectives are included for  $\text{NO}_3^{2-}$ , on  $(\text{MgO})_9$ , for the hexagonal and slab shape of  $(\text{MgO})_9$  cluster. Large spheres are represented Mg atoms; small spheres are denote O atoms, whereas dark spheres are N atoms.

and binding energies are also illustrated in (Table- 1), for  $(\text{MgO})_4$ ,  $(\text{MgO})_6$  and  $(\text{CaO})_4$  clusters.

The exotic natures of both  $\text{NO}_2$  (ads) species discussed in the present study imply the need for additional calculations in order to establish the qualitative understanding which has emerged regarding the mentioned species.

These limited variations in stability of the  $\text{NO}_3^{2-}$  species, are consistent with what was found for  $\text{NO}_2^-$  species, that make the nitrite stability change upon switching cations stand out. It is suggested that the electropositivity property is more sensitive to cation radius for adsorption at the cation positions than at the oxygen anion sites. This in turn implies that it is the locality and flexibility of the polar

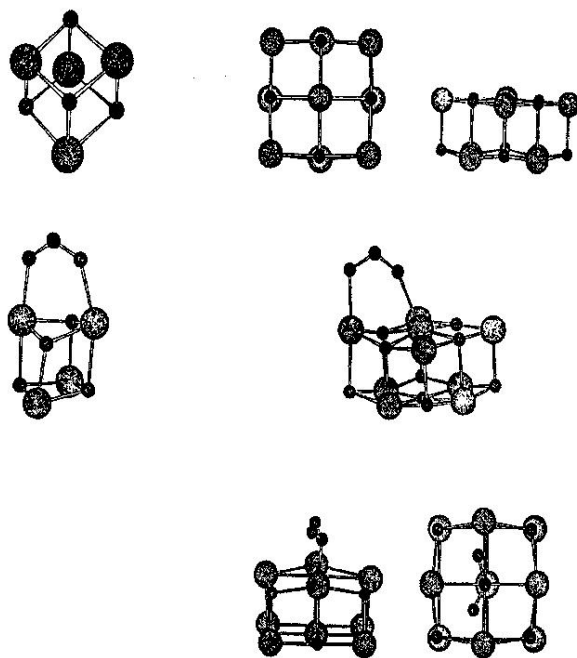


Fig. 4: Geometries and binding energies for  $\text{NO}_2 @ (\text{CaO})_n$ ,  $n = 4$  and  $9$ . Two perspectives are included for  $\text{NO}_3^{2-}$ , on  $(\text{CaO})_9$ , for the hexagonal and slab shape of  $(\text{CaO})_9$  cluster. Large spheres are represented Ca atoms; small spheres are denote O atoms, whereas dark spheres are N atoms.

covalent bonds in  $\text{O}_{\text{surf}}-\text{NO}_2^{2-}$ , which render these ions their comparable insensitivities to the choice of cation. In contrast, the energetic associated with the accommodation of a delocalized hole in an oxide cluster is found to be significantly more sensitive to the particular cation.

#### Concluding Remarks

Molecular clusters have long been understood to comprise conceptual bridges between the atom and the solid. As cluster become increasingly more relevant due to technological applications interest in the clusters and their chemistry *per se* is increasing. In a series of studies, we have focused on the alkaline earth oxides, and discussed boundary conditions related differences between cluster and bulk, it has been inferred above that substrate electropositivity would be critical property for nitrite formation at the metal ion sites.

As clusters grow, polarization forces increase and the Madelung potential of the increasingly more ionic lattice makes the substrate less reactive to electron accepting adsorbate, *i.e.* the bulk surface becomes a weaker Lewis base than the cluster. Given that the Madelung potential decreases with increasing cation radius, and taking the  $\text{O}^{2-}$  ion radius to be constant, the capability of electron pair donation increases in the series  $\text{MgO(s)} < \text{CaO(s)} < \text{SrO(s)} < \text{BaO(s)}$ .

Calculating the adsorption energies of  $\text{NO}_2$  molecules on the  $(\text{MgO})_9$  and  $(\text{CaO})_9$  clusters, we have found the bulk intuition is applicable also for clusters as the chemisorption energies increase when switching the  $\text{Mg}^{2+}$  cation for the  $\text{Ca}^{2+}$  in  $(\text{MO})_9$ , *cf.* (0.36 eV) *versus* (0.68 eV) for adsorptions to  $(\text{MgO})_9$  and  $(\text{CaO})_9$ , respectively, towards formation of surface  $\text{NO}_3^{2-}$ . Also the same thing (1.11 eV) *versus* (1.37 eV) for adsorptions to  $(\text{MgO})_4$  and  $(\text{CaO})_4$  respectively, towards formation of  $\text{NO}_2^-$ . Still, the limited differential effects seen, suggest that it is the locality aspect of the polar covalent bonding to  $\text{O}_{\text{surf}}^{2-}$ , which significantly reduced the sensitivity to choice of cation. This is contrast to the nitrite formation rout, corresponding to  $\text{NO}_2$  adsorption at cation sites. Whereas, the cluster oxygens are again the providers of the electrons, in this case the non-local nature of the delocalized hole (Fig. 2 (a)) is the cause of the significantly increased sensitivity, *i.e.* the nitrite stabilities on  $(\text{MgO})_9$  and  $(\text{CaO})_9$  come out at (0.36 eV) *versus* (1.66 eV), respectively. It is interesting to note how the nitrite formation on  $(\text{MO})_4$  come out rather similar for the two cations, while we observe that the discrepancy increases with increasing cluster size. This is again as would be expected based on differential effect upon cluster growth (see above this section).

Two types of surface nitrite and nitrate are distinguished. This concluded that, in the absence of Madelung potential, as in the case for clusters, the Lewis basicities at the  $\text{O}_{\text{surf}}^{2-}$  sites display similar strengths irrespective of the different alkaline earth cations. This is in contrast to the Lewis acidity property of the  $\text{M}^{2+}$  sites, where significant differences were observed for  $\text{NO}_2$  adsorption as a nitrite, *i.e.* adsorption involving electron transfer in conjunction to binding to cation sites.  $\text{NO}_2$  chemisorption to a closed shell  $(\text{MO})_n$  cluster involves the issue of where to accommodate the odd electron. When this oxidizing agent forms a nitrite at

the  $M^{2+}$  sites, the odd electron becomes a delocalized electron vacancy (hole) among cluster oxygens and adsorbate. In contrast, when  $NO_2$  attacks at an  $O^{2-}_{surf}$  site, two possibilities can be envisaged, in that either  $NO_3^-$  is formed in conjunction with a delocalized electron, or the unpaired electron remains on the adsorbate, resulting in a formal  $NO_3^{2-}$  surface species. The latter was found, and might be that this  $NO_3^{2-}$  transient is a missing link in the lean burn catalysis  $NO_2$  storage.

#### References

1. M. Shelef, *Chemical Reviews*, **95**, 209 (1995).
2. H. Shinjoh, N. Takahashi, K. Yokota, and M. Sugiura, *Applied Catalysis B: Environmental*, **15**, 189 (1998).
3. N. Takahashi, H. Shinjoh, T. Iijima, T. Suzuki, K. Yamazaki, K. Yokota, H. Suzuki, N. Miyoshi, S. - ichi Matsumoto, T. Tanizawa, T. Tanaka, S. - shi Tateishi, and K. Kasahara, *Catalysis Today*, **27**, 63 (1996).
4. M. Miletic, J. L. Gland, K. C. Hass, and W. F. Schneider, *Surface Science*, **546**, 75 (2003).
5. E. Fridell, H. Persson, B. Westberg, L. Olsson and M. Skoglundh, *Catalysis Letters*, **66**, 71 (2000).
6. C. Di Valentin, A. Figini, and G. Pacchioni, *Surface Science*, **556**, 145 (2004).
7. A. Satsuma, R. Akahori, M. Kato, S. Komai, H. Yoshida, and T. Hattori, *Journal of Molecular Catalysis A: Chemical*, **155**, 81 (2000).
8. A. Snis and I. Panas, *Surface Science*, **412-413**, 477 (1998).
9. W. F. Schneider, K. C. Hass, M. Miletic, and J. L. Gland, *Journal of Physical Chemistry B*, **106**, 7405 (2002).
10. H. Grönbeck, *Journal of Physical Chemistry B*, **110**, 11977 (2006).
11. H. Grönbeck, P. Broqvist, and I. Panas, *Surface Science*, **600**, 403 (2006).
12. M. M. Branda, C. D. Valentin, and G. Pacchioni, *Journal of Physical Chemistry B*, **108**, 4752 (2004).
13. L. Cheng and Q. Ge, *Surface Science Letters*, **601**, L65 (2007).
14. F. Bawa and I. Panas, *Physical Chemistry Chemical Physics*, **3**, 3042 (2001).
15. F. Bawa and I. Panas, *Physical Chemistry Chemical Physics*, **4**, 103 (2002).
16. A. D. Becke, *J. Chemical Physics*, **98**, 5648 (1993).
17. C. Lee, W. Yang and R. G. Parr, *Physical Review B*, **37**, 785 (1988).
18. S. H. Vosko, L. Wilk and M. Nusair, *Canadian Journal of Physics*, **58**, 1200 (1980).
19. M. J. Frisch, G. W. Trucks, H. B. Schlegel, G. E. Scuseria, M. A. Robb, J. R. Cheeseman, M. C. Strain, J. C. Burant, R. E. Stratmann, S. Dapprich, K. N. Kudin, J. M. Millam, A. D. Daniels, G. A. Petersson, J. A. Montgomery, V. G. Zakrewski, K. Raghavachari, P. Y. Ayala, Q. Cui, K. Morokuma, J. B. Foresman, J. Cioslowski, J. V. Ortiz, V. Barone, B. B. Stefanov, G. Liu, A. Liasshenko, P. Piskorz, W. Chen, M. W. Wong, J. L. Andres, Replogle, R. Gomperts, R. L. Martin, D. J. Fox, T. Keith, M. A. Al-Laham, A. Nanayakkara, M. Challacombe, C. Y. Peng, J. P. Stewart, C. Gonzalez, M. Head-Gordon, P. M. W. Gill, B. G. Johnson, and J. A. Pople, *Gaussian 98*, Gaussian, Inc., Pittsburgh, PA, (1998).
20. I. Panas, and A. Snis, *Theoretical Chemistry Accounts*, **97**, 232 (1997).